Bull. Chem. Soc. Jpn., *63*, *192—198 (1990)* [Vol. 63, No. 1

Activation Process of CuY Zeolite Catalyst Observed by TPR and EXAFS Measurements

Shuji TANABE and Hiroshige MATSUMOTO*
Department of Chemistry, Faculty of Liberal Arts, Nagasaki University, Bunkyomachi 1-14, Nagasaki 852
(Received July 15, 1989)

EXAFS measurements have been employed to investigate structural changes of Cu species in Y-zeolite during TPR process. The formation of an active species by a consecutive reduction-reoxidation treatment was clearly demonstrated in the TPR spectra. Detailed analysis of the EXAFS data suggested that at a considerably low temperature the active species was reduced directly to Cu metal with a particle size of 5—8 Å, while at higher temperatures the original Cu^{2+} ions were reduced by a two-step mechanism, via Cu^+ ions to Cu metal. From these points of view, the active species is considered to be small clusters of CuO with several Cu atoms.

The redox behavior of Cu^{2+} ions in zeolites has been the subject of numerous studies during the last two decades. The oxidation state of the metal component is one of the most important factors in oxide catalysts, since the quality and quantity of the active species depend strongly on the process of oxidation prior to catalysis. Cu-exchanged zeolites have been known as highly active catalysts in oxidation reactions. Their activities are closely related to the oxidation state of the Cu species, which has been characterized using various physicochemical techniques.[1-5)]

Among these techniques the temperature-programmed reduction (TPR) is considered to be one of the simplest method in studies of the reduction mechanism of the Cu species in zeolite, as shown elsewhere.[6-9)] Petunchi et al.[10)] and Miro et al.[11)] investigated the redox characteristics of Cu-zeolites by TPR experiments and showed that the cyclic treatment with CO and oxygen at high temperatures above 1000 K resulted in irreversible formation of large CuO crystals outside of the framework. Herman et al.[12)] reported, on the other hand, that the Cu metal on the internal surface of a CuY zeolite could be reoxidized back to Cu^{2+} ions located at the original sites in the lattice.

In the present work, the structural changes of the Cu species in Y-zeolite have been followed by the measurements of the K-edge extended X-ray absorption fine structure (EXAFS) i.e., the characterization of CuY zeolite activated by a consecutive reduction-reoxidation (R–O) treatment has been made by the EXAFS measurements in the sequence of each step during the course of the TPR process. The particle sizes of Cu species formed in the sample with R–O treatment are so small that conventional techniques, such as X-ray diffraction spectroscopy (XRD) and transmission electron microscopy (TEM),[6,7)] are unsuitable to investigate them. The EXAFS spectroscopy is well suited for this purpose since it can follow changes of local structure around Cu atoms.

Experimental

The CuY zeolite used in this work was prepared by the conventional method from pure crystalline Linde Y molecular sieves using copper(II) acetate (analytical reagent grade). The ion exchange was conducted overnight at pH=5.5—5.8. The exchanged sample was then washed with deionized water, air dried, pelletized, sieved and stored over saturated ammonium chloride solution. The analysis by atomic absorption revealed that 59.6% of Na^+ ions were replaced by Cu^{2+} ions by this procedure.

The TPR measurements were performed in a conventional circulation system[7)] consisting of a quartz U-type reactor, a high speed circulation pump, liquid-nitrogen trap and a pressure transducer (MKS-222B) connected with a microcomputer. The hydrogen consumption during the TPR process was estimated from the pressure decrease in this apparatus by which the pressure change corresponding to 1 μmol could be detected. Prior to each TPR measurement, the sample was evacuated for 30 min at desired temperatures to remove possible impurities and to control the adsorbed water on the surface. In the TPR measurement, extra pure hydrogen was introduced onto a small aliquot (0.6 g) of the sample (20—40 mesh) under the initial pressure of 10.0 kPa and the temperature of the reactor was raised linearly at a rate of 5 K min^{-1}.

The activation of the CuY zeolite was performed by the R–O treatment in the same system. It consists of three consecutive stages, evacuation, reduction, and reoxidation. At the desired temperatures, the zeolite was evacuated for 0.5 h, reduced with 10 kPa pressure of hydrogen for 2 h and reoxidized with 10 kPa pressure of oxygen for 2 h.

Details of the EXAFS instrument employed in this work has been described elsewhere.[13-15)] Basically it consists of a rotating anode X-ray generator (Rigaku Ru-200), a spectrometer with a bent silicon (220) crystal of Johansson cut, ion chambers, slits and counting electronics, which are controlled by a computer through a CAMAC bus. The X-ray source with a silver target was operated at 14 kV and 200 mA to minimize the effect of higher order reflections on the ion chamber. The CuY samples, pressed into thin wafers, were treated similarly to the TPR and R–O treatment.

A detailed method of data analysis also has been described elsewhere.[13-15)] A single scattering model for EXAFS oscillations expressed by[16,17)]

$$\chi(k) = \sum_j \frac{N_j}{kR_j^2} \exp[-2(\sigma_j^2 k^2 + R_j/\lambda)] \times F_j(\pi, k) \sin(2kR_j + \alpha_j(k)) \qquad (1)$$

where k is the photoelectron wave vector, R_j is the distance from the central Cu atoms to atoms in the jth shell, N_j is the coordination number of the central atoms, F is the scattering amplitude, σ_j is the Debye–Waller factor, and α_j is the phase shift. The mean free path of the photoelectron in the solid, λ, was assumed to be independent of k in this analysis. The EXAFS function was Fourier transformed by weighting k^3 to yield the radial distribution function, $\Phi(R)$, as follows.

$$\Phi(R) = (1/2)^{1/2}\int k^3\chi(k)\exp(-2\pi kR)\mathrm{d}k \qquad (2)$$

The curve-fitting procedures were employed to determine structural parameters, such as R and N. The main peaks in the radial distribution functions were back-transformed into k space and a least-squares calculations were made by using Eq. 1.

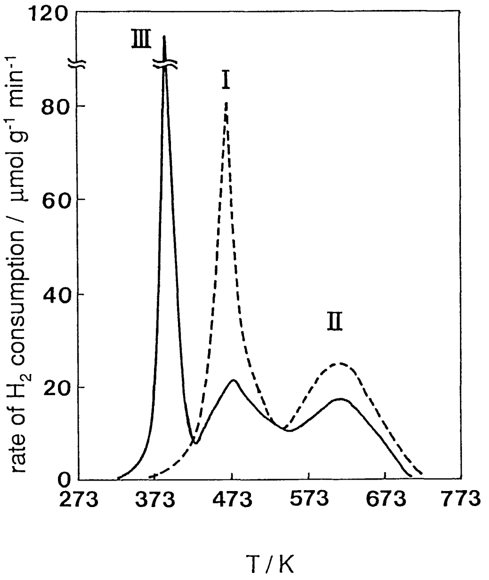

Fig. 1. TPR sepectra for CuY before (broken curve) and after (solid curve) the R–O treatment (evacuated at 523 K, reduced at 673 K and reoxidized at 473 K).

Results

It is already known that the reduction of Cu^{2+} ions in zeolites occurs by a two-step mechanism, via Cu^+ ions to Cu metal.[18] The two-step reduction could be demonstrated directly in the TPR spectra measured under suitable conditions, such as a low temperature in the preliminary evacuation of the sample, a low pressure of hydrogen in the system and a slow rate of the temperature increment. Representative TPR spectra are shown in Fig. 1. The broken curve indicates the rate of hydrogen consumption by the original CuY zeolite evacuated at 523 K. The spectrum consists of two distinct peaks with maxima around 460—470 and 620—630 K. During the TPR process, the greenish blue sample turned white when the first peak appeared, and then it turned pink above 600 K. The first peak (I) is associated with the reduction of Cu^{2+} to Cu^+ ions, while the second peak (II) is due to that of Cu^+ ions to Cu metal. This mechanism was first proposed by Jacobs et al.[18] and confirmed by electron spin resonance (ESR) and infrared (IR) spectra in our previous report.[7]

When the reduced sample was reoxidized during the course of the R–O treatment, it changed from pink to light gray in color. At the same time, the ESR signal due to Cu^{2+} ions was appreciably reduced in intensity, suggesting that during the R–O treatment the paramagnetic Cu^{2+} ions in the zeolite converted to an ESR-insensitive species, such as CuO or Cu_2O. After the R–O treatment, however, the formation of such oxides could not be recognized in the sample by XRD measurement.

The TPR profile of CuY with the R–O treatment is shown by the solid curve in Fig. 1. In this spectrum a new sharp peak (III) of hydrogen consumption is observed at a low temperature around 390 K in addition to peaks I and II, i.e., an easy-reducible

Table 1. Effects of Evacuation, Reduction, and Reoxidation Stages during the R–O Treatment on the Formation of the Active Species X

	Treatment/K			H_2 consumption/mmol g^{-1}	
	Evac[a]	Redn[b]	Oxin[c]	Species X	Total
Effect of evacuation	293	673	673	0.12	0.75
	523	673	673	0.38	0.97
	573	673	673	0.27	0.94
	673	673	673	0.22	0.91
	773	673	673	0.05	0.62
Effect of reduction	523	573	473	0.19	1.08
	523	673	473	0.49	1.07
	523	773	473	0.15	0.79
Effect of reoxidation	523	673	473	0.49	1.07
	523	673	573	0.49	1.06
	523	673	673	0.38	0.97

Treatments at each stage were performed for a), 0.5 h; b), 2 h; c), 2 h.

species (X) formed in the zeolite during the R–O treatment. The formation of species X markedly depends on the condition of each stage in the R–O treatment, such as preliminary evacuation, reduction with hydrogen and reoxidation with oxygen. In order to determine the effects of temperature in these stages on the formation of species X, the amount of species X is estimated from the area of peak III in the TPR spectra. The results are summarized in Table 1, together with the total amounts of hydrogen consumption through the TPR process up to 723 K. The hydrogen consumptions for the peaks I and II in the TPR spectra could not be estimated separately, since these peaks were broad and unresolved in the case of samples evacuated at higher temperatures.

Among each stage in the R–O treatment the evacuation stage shows the most significant influence for the formation of species X, i.e., the lower the temperature in the evacuation, the more preferential it is for the formation of species X. It is speculated that a small quantity of water is needed as a preferential condition of the subsequent reduction stage, since appreciable amounts of water are considered to be still adsorbed on the zeolites evacuated at lower temperatures.[19,20] The role of water in the reduction stage was qualitatively confirmed by the introduction of water to the system. For example, when in the reduction stage water at 2.0 kPa pressure was introduced onto the sample evacuated at high temperature of 773 K, the amount of species X formed after the reoxidation increased remarkably, as is depicted in Fig. 2. Recently, Sano et al.[21] have recognized in their detailed EXAFS study that the reducibility of a nickel-exchanged Y zeolite is markedly improved by soaking the sample in an aqueous NaOH solution. It has been reported by Naccache et al.,[22] furthermore, that the reduction of Cu^{2+} ions in CuY is promoted by the presence of water via the formation of $Cu(OH)^+$ ions as the intermediate.

In the effect of reduction temperature in the R–O treatment, the maximum formation of species X was obtained at 673 K. At lower temperatures in the reduction stage it is discernible from Table 1 that much of the Cu species is reoxidized back to Cu^{2+} ions after the reoxidation. Accordingly the formation of Cu metal, which will prevent such reversible redox cycle, is considered to be necessary for the formation of species X. The reoxidation stage, on the other hand, scarcely affects the formation of species X. In the temperature-programmed oxidation spectra of the sample reduced at various temperatures, only one sharp peak was observed at a low temperature around 470 K, indicating a high velocity for the reoxidation stage in this system. In summary, the optimum temperatures in the activation of CuY zeolite are determined to be 523, 673, and 473 K, respectively, for the evacuation, reduction, and reoxidation stages during the R–O teatment tested in the present investigation.

Measurements of EXAFS spectra were performed to investigate the changes of the Cu species in the zeolite. The spectra were measured in the sequence of each step during the course of the R–O treatment and the TPR process. Fourier transforms to real space of the obtained EXAFS spectra, the $\Phi(R)$ function of Eq. 2 are shown in Figs. 3—6. In these figures the peaks are displaced slightly from the true interatomic distances

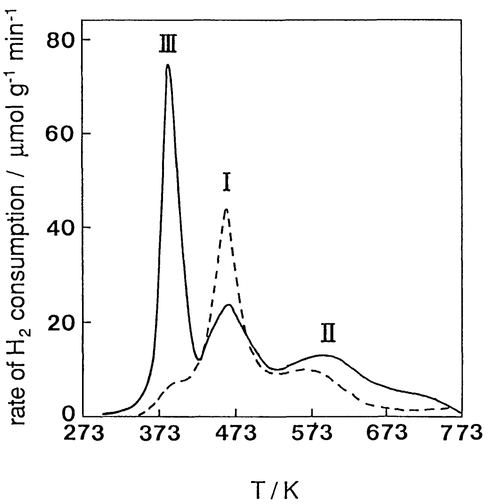

Fig. 2. TPR spectra for the activated CuY (evacuated at 773 K, reduced at 673 K and reoxidized at 673 K) in the presence (solid curve) and absence (broken curve) of water during the reduction stage.

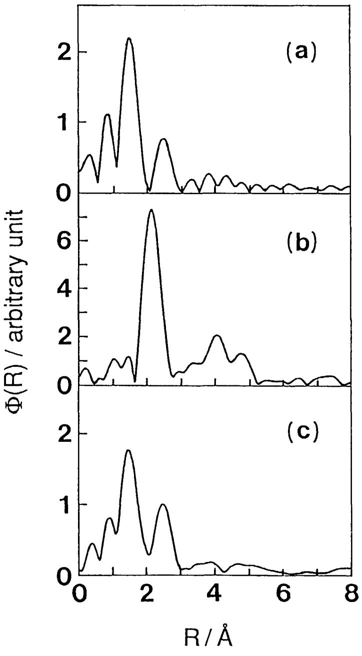

Fig. 3. Fourier transforms of EXAFS spectra for CuY during the R–O treatment in the sequence of evacuation at 423 K (a), reduction at 673 K(b), and reoxidation at 473 K(c).

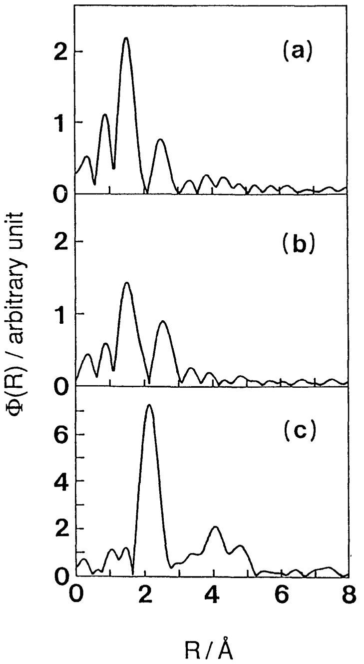

Fig. 4. Fourier transforms of EXAFS spectra for CuY without the R-O treatment in the course of TPR process. Reduction temperature; 423 K(a), 523 K(b), and 673 K(c).

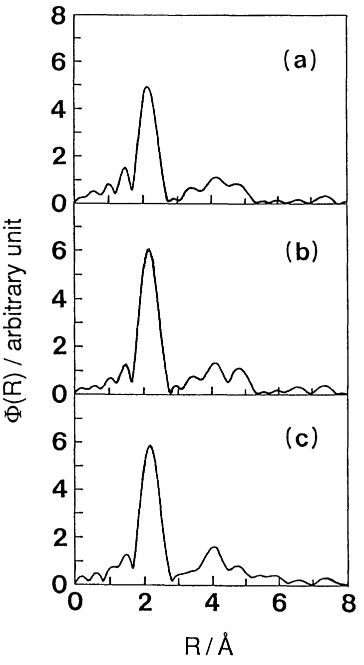

Fig. 5. Fourier transforms of EXAFS spectra for CuY with the R-O treatment in the course of TPR process. Reduction temperature; 423 K(a), 523 K(b), and 673 K(c).

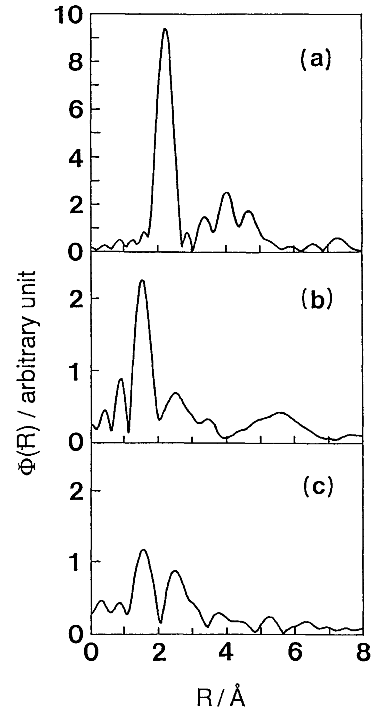

Fig. 6. Fourier transforms of EXAFS spectra for Cu foil(a), CuO powder(b) and Cu_2O powder(c).

because of the phase shift. The distances used in the text are the values after correction for the phase shift.

In the Fourier transform of the evacuated CuY zeolite (Fig. 3a) a predominant peak appears at 1.97 Å which is similar to the Cu-O distance of the shortest Cu-O bond in CuY zeolite.[23] Upon reduction of the evacuated sample at 673 K for 2 h a strong peak is observed at 2.51 Å in the radial distribution function (Fig. 3b). This agrees well with the Cu-Cu distance in Cu foil (Fig. 6a). After the reduced sample is reoxidized at 473 K for 2 h (the optimum R-O treatment) the main peak appears at 1.96 Å, as is shown in Fig. 3c. Although this value coincides well with that in the reference CuO powder (Fig. 6b), no significant difference is recognized also in comparison with that in the original sample (Fig. 3a).

During the TPR process the original CuY zeolite shows no substantial changes of the radial distribution function upon reduction up to 423 K (Figs. 3a and 4a), as is readily expected from the TPR spectrum in Fig. 1. After reduction at 523 K, where the peak I appeared in the TPR spectrum, the peak of the first neighbor shell in the Fourier transform decreases in intensity, as is shown in Fig. 4b. On further reduction up to 673 K (Fig. 4c), the peak positions and the relative amplitudes become very similar to those in the reduced sample (Fig. 3b), indicating almost complete reduction of the Cu species in the sample evacuated at the low temperature of 523 K.

In the case of CuY with the R-O treatment, on the other hand, a striking change is observed in the radial distribution function of the sample reduced at low temperature. As shown in Fig. 5a, a predominant peak appears at 2.52 Å of the Cu-Cu distance when the treated sample is reduced according to the TPR mode up to 423 K, where the peak III is supposed to have already been eliminated in the TPR spectrum (Fig. 1). The intensity of this peak slightly increases on increasing the reduction temperature up to 523 K (Fig. 5b). Further rise in the temperature, however, has no substantial effect on the radial distribution function (Fig. 5c).

Discussion

The information obtained in the analysis of the EXAFS data reflects the local structure around Cu atoms in the zeolite. In order to determine the structural basis for changes of the Cu species during the TPR process, inverse Fourier transforms have been carried out for each main peak in Figs. 3—6. The inverse Fourier transforms are compared with the calculated values of $k^3\chi(k)$ assuming the Cu–O or Cu–Cu scattering to obtain the "best-fit" curves.[12] Representative results are shown in Fig. 7. For the CuY zeolite with and without the R–O treatment, the estimated best-fit values of some structural parameters during the TPR process are summarized in Table 2, as well as those for reference materials.

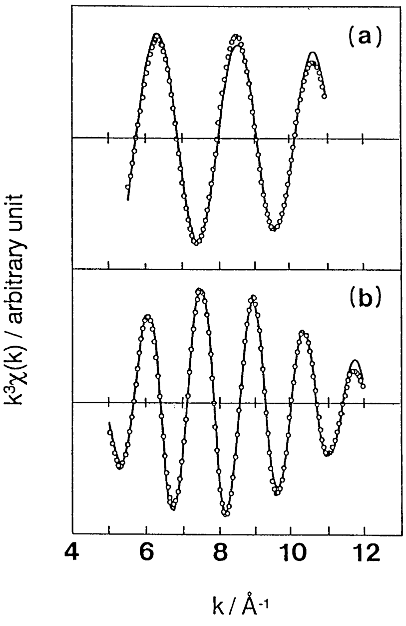

Fig. 7. Comparisons of inverse Fourier transforms (solid curves) for the main peaks in Figs. 3c(a) and 5a(b) with best-fit curves assuming the Cu–O scattering in CuO and Cu–Cu scattering in Cu foil, respectively.

Table 2. Best-Fit Values of Structural Parameters of CuY Zeolite with and without the R–O Treatment during the TPR Process

Sample	Redn/K	Bond	R/Å	N
CuY without the R–O treatment	298	Cu–O	1.97	3.7
	423	Cu–O	1.97	3.7
	523	Cu–O	1.93	2.8
	673	Cu–Cu	2.51	10.0
CuY with the R–O treatment	298	Cu–O	1.96	4.4
	423	Cu–Cu	2.52	7.0
	523	Cu–Cu	2.52	8.5
	673	Cu–Cu	2.52	8.8
Cu foil	—	Cu–Cu	2.51	12.0
CuO powder	—	Cu–O	1.96	4.0
Cu_2O powder	—	Cu–O	1.86	2.0

In the radial distribution of the original CuY evacuated at low temperature (Fig. 3a), the main peak is observed at 1.97 Å which probably corresponds to the Cu–O distance between Cu^{2+} ions and the lattice oxygen atoms in the sodalite cages of the faujasite matrix.[24,25] It is expected that a predominant portion of the Cu^{2+} ions in 59.6% exchanged CuY zeolite used in the present work are located at Site I′ in the sodalite cages.[24] These ions are considered to be coordinated with three lattice oxygen atoms.[25] The coordination number of the Cu atoms in the present sample (N=3.7) presumably indicates an average number of bare and hydrated ions in the sodalite cages. After the evacuated sample is reduced at 523 K, where most Cu^{2+} ions transform into Cu^{+} ions (Fig. 1), the coordination of Cu atoms decreases significantly whereas the Cu–O distance remains unchanged. Discussion of these values cannot be made here, unfortunately, because of the lack of detailed information about the location of the Cu^{+} ions in the Y-zeolite. In the sample reduced at 673 K the coordination of N=10.0 is slightly smaller than that in Cu foil (N=12.0), while the Cu–Cu distances show good agreement.

Upon R–O treatment, on the other hand, the original Cu^{2+} ions are expected to convert into another Cu species, as observed in the TPR spectrum (Fig. 1). The calculated curve for the main peak in Fig. 3c, assuming the Cu–O scattering in CuO, well reproduces the inverse Fourier transforms (Fig. 7a). Between the samples before and after the R–O treatment, however, no appreciable difference in the Cu–O distance is observed, while the coordination of the Cu atoms is increased from 3.7 to 4.4 by this treatment.

After reduction of CuY with the R–O treatment at 423 K, where the peak III has been eliminated from the TPR spectra (Fig. 1), the calculated curve for the main peak in Fig. 5a, assuming the Cu–Cu scattering in Cu metal, reproduces completely the obtained inverse Fourier transforms (Fig. 7b). It clearly shows the dramatic influence of the R–O treatment, since in the case of the original CuY no changes are observed in the EXAFS and TPR experiments by the reduction at this temperature. That is, the species X is reduced directly to Cu metal at a low temperature, while the original Cu^{2+} ions in the zeolite are reduced at much higher temperatures by the two-step mechanism.

In comparison with the infinite crystals (N=12.0), however, the metal formed from the species X exhibits extremely small coordination which increases slightly with the rise in reduction temperature (N=7.0 to 8.8). The discrepancy between these values is mainly attributed to the difference in the size of Cu metal, i.e., the coordination number in small particles is smaller than that in large crystals because of the high proportion of surface atoms.[26,27] Applying the theory by Greegor and Lytle[28] to the present system and assuming a sphere shape of the particles, the average particle size of the Cu metal formed by reduction of the species X is estimated to be 5—8 Å. This is distinctly smaller than the main cavity size of the faujasite framework (ca. 12 Å).

When CO was adsorbed on CuY reduced at 523 K, an intense absorption band appeared around 2160 cm^{-1} in the IR spectrum.[7] This band is attributed to the Cu^{+}-CO complex in the super cages.[12,18] After reduction of CuY with the R–O treatment at 423 K, however, no distinct band was observed in this wavenumber region. Furthermore, the species X showed no ESR signal due to Cu^{2+} ions, as described above. These observations suggest that the species X is not isolated Cu^{2+} ions but a covalent-bonded oxide, such as CuO or Cu$_2$O. Petunchi et al.[8] and Miro et al.[9] have already recognized by XRD measurement that CuO crystals form in Cu-zeolites after cyclic treatments with CO and oxygen at an extremely high temperature of 1023 K. However, no XRD pattern of CuO or Cu$_2$O was observed in CuY with the R–O treatment.

In order to make a clear identification of the species X, the extracted oscillation of the observed EXAFS spectrum of CuY with the R–O treatment is compared with those of possible oxides in Fig. 8. It can be concluded from the detailed comparison of these oscillations that CuY with the R–O treatment bears a closer resemblance to CuO rather than to Cu$_2$O. In the TPR spectra by the similar procedure, furthermore, bulk CuO powder or finely dispersed CuO on SiO$_2$ exhibited a single broad peak of hydrogen consumption with maximum around 680 or 430 K, respectively. This might indicate that the peak temperature in the TPR spectrum increased with the increase in the particle size of the CuO. From this point of view, it is plausible that the species X is CuO clusters and is so small as to escape XRD measurement.

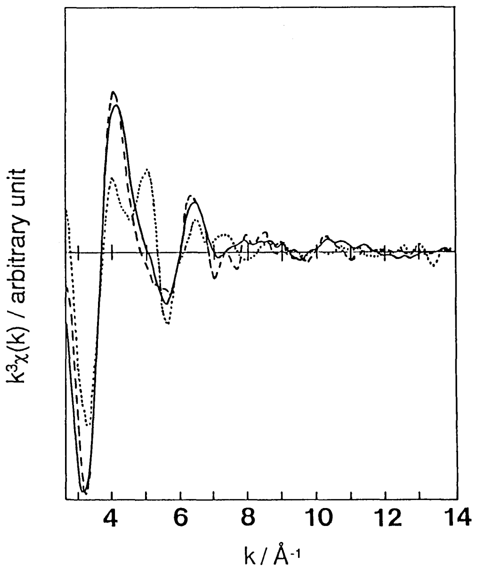

Fig. 8. Comparisons of extracted oscillations of the observed EXAFS spectra for CuY with the R–O treatment (solid curve), CuO (broken curve), and Cu$_2$O (dotted curve).

After reduction of CuY with the R–O treatment at 423 K (the sample in Fig. 5a) it was again reoxidized with oxygen at the same temperature and the TPR was then performed in a similar manner. This reoxidized sample showed a TPR spectrum resembling closely that of CuY with the standard R–O treatment. Furthermore, the Cu species in this sample transformed into Cu metal with R=2.52 Å and N=7.0 upon the second reduction at 423 K. From this reversible behavior, it can be presumed that the number of Cu atoms in the metal clusters is substantially retained during the redox cycle at 423 K. Therefore, the species X, the precursor of the metal clusters, is considered to be small CuO clusters with several Cu atoms.

In this work, the changes of the Cu species during the R–O treatment and TPR process have been investigated by the analysis of EXAFS data only for the nearest neighboring atoms. Further analysis for outer shells is needed to explain the detailed structure of these clusters.

In summary, the results of the present study demonstrate the formation and characterization of an active species in CuY zeolite. The active Cu species is formed by a consecutive reduction-reoxidation treatment under very mild conditions. The active species, which was considered to be small CuO clusters, was directly and reversibly reduced to Cu metal clusters at a considerably low temperature, while the original Cu^{2+} ions in the zeolite were reduced by the two-step mechanism, via Cu^{+} ions to Cu metal at higher temperatures.

The authors express their gratitude to Drs. Yasuo Udagawa, Kazuyuki Tohji, and Mr. Takanori Mizushima (Institute for Molecular Science, Okazaki) for their helpful supports in EXAFS experiments and analysis.

References

1) R. A. Schoonhydt, L. J. Vandamme, P. A. Jacobs, and J. B. Uytterhoeven, *J. Catal.*, **43**, 292 (1976).

2) F. D. Bravo, J. Bwyer, and D. Zamboulis, "The Properties and Applications of Zeolites," ed by R. P. Townsend, Chem. Soc., London, (1979), p. 369.

3) N. S. Mcintyer, S. Sunder, D. W. Shoesmith, and F. W. Stanchell, *J. Vac. Sci. Technol.*, **18**, 714 (1981).

4) H. Chon, G. Seo, and B. J. Ahn, *J. Catal.*, **80**, 90 (1983).

5) M. Narayana, S. Contarini, and L. Kevan, *J. Catal.*, **94**, 370 (1985).

6) S. Tanabe and H. Matsumoto, *Chem. Lett.*, **1985**, 1425.

7) S. Tanabe and H. Matsumoto, *Appl. Catal.*, **45**, 27 (1988).

8) S. Tanabe and H. Matsumoto, *Chem. Lett.*, **1989**, 539.

9) H. Matsumoto and S. Tanabe, *J. Chem. Soc., Chem. Commun.*, **1989**, 875.

10) J. O. Petunchi and W. K. Hall, *J. Catal.*, **80**, 403 (1983).

11) E. E. Miro, D. R. Ardiles, E. A. Lombardo, and J. O. Petunchi, *J. Catal.*, **97**, 43 (1986).

12) R. G. Herman, J. H. Lunsford, H. K. Beyer, P. A. Jacobs, and J. B. Uytterhoeven, *J. Phys. Chem.*, **79**, 2388 (1975).

13) K. Tohji, Y. Udagawa, S. Tanabe, T. Ida, and A. Ueno, *J. Am. Chem. Soc.*, **106**, 5172 (1984).

14) K. Tohji, Y. Udagawa, S. Tanabe, and A. Ueno, *J. Am. Chem. Soc.*, **106**, 612 (1984).

15) K. Tohji, Y. Udagawa, T. Mizushima, and A. Ueno, *J. Phys. Chem.*, **89**, 5671 (1985).

16) E. A. Stern, *Phys. Rev. B*, **10**, 3027 (1974).

17) E. A. Stern, D. E. Sayers, and F. W. Lytle, *Phys. Rev. B*, **11**, 4836 (1985).

18) P. A. Jacobs, J. P. Linert, H. Nijs, and J. B. Uytterhoeven, *J. Chem. Soc., Faraday Trans. 1*, **73**, 1745 (1977).

19) J. W. Word, *J. Catal.*, **11**, 238 (1968).

20) H. Matsumoto, H. Futami, F. Kato, and Y. Morita, *Bull. Chem. Soc. Jpn.*, **44**, 3170 (1971).

21) M. Sano, T. Maruo, H. Yamatera, M. Suzuki, and Y. Saito, *J. Am. Chem. Soc.*, **109**, 52 (1987).

22) C. M. Naccache and Y. B. Taarit, *J. Catal.*, **22**, 171 (1971).

23) P. Gallezot, Y. B. Taarit, and B. Imerik, *J. Catal.*, **26**, 295 (1975).

24) P. Gallezot, Y. B. Taarit, and B. Imerik, *Compt. Rend.*, **C272**, 261 (1971).

25) C. C. Chao and J. H. Lunsford, *J. Chem. Phys.*, **57**, 1890 (1972).

26) D. R. Denley, R. H. Raymond, and S. C. Tang, *J. Catal.*, **87**, 414 (1984).

27) P. W. J. G. Wijnen, F. B. M. Van Zon, and D. C. Koningsberger, *J. Catal.*, **114**, 463 (1988).

28) R. B. Greegor and F. W. Lytle, *J. Catal.*, **63**, 476 (1980).